Journal of Molecular Catalysis B: Enzymatic 83 (2012) 125–130

Contents lists available at SciVerse ScienceDirect

Journal of Molecular Catalysis B: Enzymatic

journal homepage: www.elsevier.com/locate/molcatb

Monolayer properties of synthesized tyrosyl esters

Imen Aissa [a], Julien Leclaire [b], Yassine Ben Ali [a], Fakher Frikha [a], Youssef Gargouri [a,*]

[a] Laboratory of Biochemistry and Enzymatic Engineering of Lipases, ENIS route of Soukra, P.O. Box 1173, 3038 University of Sfax, Tunisia
[b] Laboratoiry of chirosciences, Institute of Molecular Sciences of Marseille UMR 6263, Scientific Campus of St Jérôme,13397 Marseille cedex 20, France

ARTICLE INFO

Article history:
Received 20 December 2011
Received in revised form 6 July 2012
Accepted 11 July 2012
Available online 20 July 2012

Keywords:
Tyrosol
Immobilized lipases
Monomolecular film
Critical surface pressure
Phospholipid monolayer

ABSTRACT

Lipase-catalyzed synthesis of eight fatty acid tyrosyl esters (**TyC_2** to **$TyC_{18:1}$**) was investigated using non commercial lipases from *Rhizopus oryzae* and *Staphylococcus xylosus* immobilized onto $CaCO_3$. The monomolecular film technique was used to compare the ability of the various synthesized tyrosyl fatty acid esters to form a stable monolayer at the air/water interface and their capacity to interact with a phospholipid monolayer. The measurements of surface pressure versus the molecular area shows that, in contrast to tyrosol esterified with short and medium chains (acetic (**TyC_2**), propionic (**TyC_3**), caprylic (**TyC_8**) and capric (**TyC_{10}**) acids), tyrosol esterified with long chains: lauric (**TyC_{12}**), palmitic (**TyC_{16}**), stearic (**TyC_{18}**) and oleic (**$TyC_{18:1}$**) acids are able to form a stable monolayer at the air/water interface. A direct correlation was observed between the length of the saturated acyl chain of the derivatives and their corresponding collapse pressures. The presence of unsaturation reduces the collapse pressure value. The interaction of tyrosyl esters with a phospholipid monolayer was studied and the critical surface pressure (π_c) of each ester was determined. Only medium and long chain (**TyC_8** to **$TyC_{18:1}$**) derivatives esters were found to interact efficiently with $DiC_{12}PC$ film.

1. Introduction

The disruption of biological membranes by amphiphilic molecules has been a frequent focus for study because of its applicability to basic science as well as widespread human use [1]. Because their perturbation is directed by physicochemical processes, model membrane systems can provide valuable information that would be difficult to attain *in vivo*. Monolayers offer several key advantages over other membrane models. A monolayer can be carefully controlled by defining molecular density on a Langmuir film balance. The penetration of amphiphile compounds inside insoluble monolayers has been extensively studied from a thermodynamic perspective, providing a valuable tool to examine the interaction between the amphiphile surfactant and the phospholipid or lipid monolayer [2]. Phenolic derivatives are a class of amphiphilic compounds characterized by their antioxidant activity in food matrices. The amphiphilic character of these recently called "phenolipids" may generate certain surface-active properties that would lead to a non-ionic surfactant [3].

Tyrosol [2-(4-hydroxyphenyl) ethanol], is a well-known monophenolic antioxidant present in large amount in olive oil [4]. Its efficiency was demonstrated in inhibiting the oxidation of cholesterol in LDL and preventing the modification of the apoproteic moiety [5]. Tyrosol has been also effective in inhibiting leukocyte 5-lipooxygenase [6] and protecting the Caco-2 intestinal mucosa cells against the cytostatic and cytotoxic effects produced by oxidized LDL [7]. Many other activities of tyrosol were described, such as its ability to inhibit ADP-induced platelet aggregation [8], to significantly reduce the arrhythmic activity that occurs during myocardial ischemia and reperfusion [9], and to possess significant neuroprotective activities against glutamate-induced neurotoxicity in primary cultures of rat cortical cells and injury induced by 5-S-cysteinyl-dopamine in vitro [10]. Lipophilic derivatives of tyrosol and, in particular, esters bearing acyl chains exhibit a better affinity with lipophilic membrane constituents. Then, these compounds could play an important role in pharmaceutical and cosmetic fields [11]. In the last decade, growing attention has been devoted to the synthesis of tyrosyl esters derived from fatty acids. Short, medium and long chain derivatives of the tyrosol were synthesized by transesterification reactions using lipases [12,13]. Amphiphilic tyrosol derivatives display particularly interesting characteristics, resulting from the modification of their molecular flexibility. Recently, Lucas et al, have reported that the tyrosol acyl chains derivatives are a relevant surfactant [14]. Compared to tyrosol, the presence of the acyl chains result in a substantial

Abbreviations: TyC_2, tyrosyl acetate; TyC_3, tyrosyl propionate; TyC_8, tyrosyl caprylate; TyC_{10}, tyrosyl capriate; TyC_{12}, tyrosyl laurate; TyC_{16}, tyrosyl palmitate; TyC_{18}, tyrosyl stearate; $TyC_{18:1}$, tyrosyl oleate; SXLi, immobilized *Staphylococcus xylosus* lipase; ROLi, immobilized *Rhizopus oryzae* lipase; $CaCO_3$, calcium carbonate; LC–MS, high performance liquid chromatography coupled to mass spectrometry; ABTS, 2,2-azino-bis-3-ethylbenzothiazoline-6-sulfonic acid; TEAC, trolox equivalent antioxidant capacity; $DiC_{12}PC$, 1,2-dilauryl-sn-glycero-3-phosphocholine; π_c, critical surface pressure; π_i, initial surface pressure.

* Corresponding author. Tel.: +216 74675055; fax: +216 74675055.
E-mail address: ytgargouri@yahoo.fr (Y. Gargouri).

1381-1177/$ – see front matter © 2012 Elsevier B.V. All rights reserved.
http://dx.doi.org/10.1016/j.molcatb.2012.07.002

modification of molecular packing, and thus of the monolayer properties. Therefore, the direct study of tyrosyl derivatives–lipid interactions seems to be a useful experimental approach to understand their biological effects towards various membranes.

To our knowledge, we report in this paper for the first time, a comparative study of the monolayer properties at the air/water and phospholipid/water interface of various tyrosyl fatty acid esters synthesized by a direct esterification of tyrosol with different fatty acids using non commercial lipases as biocatalyst.

2. Materials and methods

2.1. Materials

The n-hexane was purchased from Prolabo (Paris, France). The ethyl acetate was purchased from Pharmacia (Uppsala, Sweden). Caprylic, capric, palmitic, oleic acids and 2-methyl-2-propanol were purchased from Fluka (Germany), 1,2-dilauryl-sn-glycero-3-phosphocholine ($DiC_{12}PC$) was purchased from AVANTI POLAR-LIPID, Inc.

2.2. Production and immobilisation of lipase

Staphylococcus xylosus lipase and *Rhizopus oryzae* lipase were produced as described by Mosbah et al. [15] and Ben Salah et al. [16] respectively. The enzyme immobilization was made onto $CaCO_3$ as described by Ghamgui et al. [17]. The activities of the immobilised lipases were measured titrimetrically with a pH-stat, under the standard assay conditions described previously by Rathelot et al. [18] using olive oil emulsion as substrate. One international unit (UI) of lipase activity was defined as the amount of lipase that catalyses the liberation of 1 μmol of fatty acid from olive oil per minute at pH 8.5 and 37 °C.

2.3. Esterification reactions

Production of tyrosyl acetate (**TyC_2**) was performed as previously reported by Aissa et al. [12]. Tyrosyl lipophilic esters (**TyC_8** to **$TyC_{18:1}$**) were synthesized by direct esterification of tyrosol with different fatty acids in screw-capped flasks. Tyrosol (20 mg) was dissolved in 4 mL equivalent volume ratio of 2-methyl-2-propanol/n-hexane. Fatty acid concentration was adjusted to obtain tyrosol/fatty acid molar ratio of 1/8. The mixture was stirred at 45 °C in an orbital shaker at 200 rpm and in presence of 1000 UI of SXLi or ROLi. In parallel, reactions under the same conditions were conducted without enzyme. Aliquots of the mixture reaction were withdrawn at different times of incubation and filtered to be used for HPLC analysis. The conversion yield of tyrosyl derivatives was calculated as, the ratio of tyrosol number of mol converted per total number of tyrosol, using benzoic acid as internal standard.

2.4. HPLC analysis

The identification tyrosyl ester derivatives was carried out using HPLC system (Dionex, Germany).The HPLC system was equipped with a pump (LPG-3400SD), column oven and diode-array UV/VIS detector (DAD-3000RS,RI-101).The output signal of the detector was recorded using Dionex Chromeleon™ chromatography Data System. The separation was executed on a Inertsil ODS-4 C18 column (5 μm, 4.6 mm × 150 mm) maintained at 35 °C. The flow rate was 1.5 mL/min, the injection volume was 20 μL and the detection UV wavelength was set at 280 nm. The mobile phase used was 1‰ acetic acid in water (A) versus 0.5‰ acetic acid in acetonitrile (B) for a total running time of 20 min and the following proportions of solvent B were used for the elution: 0–3 min: 10–30%; 3–5 min: 30–90%; 5–18 min: 90% and 18–20 min: 90–10%.

2.5. Purification of tyrosyl derivatives

Each reaction mixture was dried and dissolved in chloroforme/acetonitrile (90/10) at a concentration of 10 mg/mL. The purification of the various tyrosyl derivatives was performed by a preparative LCMS. Experiments were carried out with a Waters 2767 LC system consisting of degasser, binary pump, auto sampler, and column heater. The column outlet was coupled to a Waters Ion Trap XCT mass spectrometer equipped with an ESI ion source. Data acquisition and mass spectrometric evaluation were carried out on a personal computer with Data Analysis software (Chemstations). For the chromatographic separation an X Bridge™ C18 Column (10 mm × 150 mm) was used. The mobile phase used was 0.5% formic acid in water (A) versus 0.5% formic acid in acetonitrile (B) for a total running time of 20 min, and the following proportions of solvent B were used for the elution: 0–2 min, 50–99%; 2–15 min, 99%; 15–17 min, 99–50%; and 17–20 min, 50%. The flow rate was 5 mL min^{-1} and the injection volume was 300 μL. Purified compound was identified by LC/MS analysis.

2.6. Measurement of the trolox equivalent antioxidant capacity (TEAC)

The ABTS radical-scavenging activity was determined according to Re et al. [19]. The ABTS radical cation was prepared by reacting an aqueous solution of ABTS (7 mM) with potassium persulfate (2.45 mM, final concentration) which was kept in dark at 25 °C for 12–16 h. The solution was diluted before use in ethanol to an absorbance of 0.70 (±0.020) at 734 nm. Aliquots of trolox or sample in ethanol (10 μL) were added into 990 μL of this diluted solution and the absorbance at 734 nm was determined at 30 °C, 6 min after initial mixing. Appropriate solvent blanks were run in each assay. The extent of decolorization was estimated by monotering the reduction of the absorbance at 734 nm. The antioxidant activity was determined as a function of compounds and calculated relative to the equivalent trolox concentration. The activity of each antioxidant was determined at three concentrations, within the range of the dose–response curve of trolox and the radical-scavenging activity was expressed as the trolox equivalent antioxidant capacity (TEAC), defined as mM of trolox.

2.7. Monolayer study of the tyrosyl derivatives

Experiments were carried out on KSV 2200 Barostat equipment. Teflon trough equipped with two hydrophilic Delrin barriers (symmetric compression) and a Wilhelmy plate as a surface-pressure sensor. Software KSV 2200 was used to control the experiments. Before each utilization, the Teflon trough was cleaned with tap water, then gently brushed in the presence of distilled ethanol, subsequently washed again with tap water, and finally rinsed with double-distilled water.

The aqueous subphase (buffer A) was composed of 10 mM Tris–HCl, pH 8, 100 mM NaCl, 21 mM $CaCl_2$, and 1 mM EDTA. Buffer was prepared with double-distilled water and filtered through a 0.45 μM Millipore filter. Residual surface active impurities were removed before each assay by sweeping and suction of the surface [20].

2.7.1. Force/area curves of tyrosol and its acyl chain derivatives

The surface pressure was measured with a Wilhelmy plate (perimeter 3.94 cm) attached to an electromicrobalance, which was connected in turn to a microprocessor programmed to regulate the movement of the mobile barrier. Tyrosol derivatives solutions

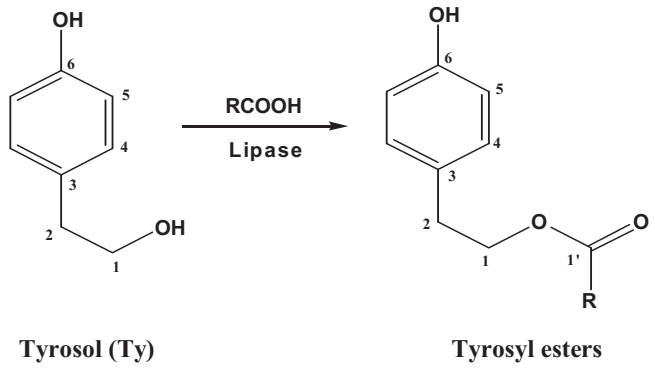

Fig. 1. Structure of the synthesized compounds.

were prepared by dissolving the compounds in pure $CHCl_3$ at a final concentration of 1 mg mL^{-1}. 50 μL of each compound was spread over an aqueous subphase (buffer A) using microliter™ syringes (HAMILTON Bonaduz AG,Switzerland) and a Teflon trough (Surface area, 352.24 cm^2).

The film was then compressed at a constant rate of 20 mm min^{-1} [21].

2.7.2. Measurement of the tyrosol derivatives penetration into $DiC_{12}PC$ monolayer

The surface pressure increase, due to the penetration of the tyrosol derivatives into the $DiC_{12}PC$ monolayer, was measured in a cylindrical trough drilled into a Teflon block (surface area 17.42 cm^2, total volume 15 mL). The aqueous subphase (buffer A) was stirred continuously at 250 rpm with a magnetic rod. The critical surface pressures were determined as described previously [21]. A sample of tyrosol or synthesized ester solution (0.5 μM) was injected under a monomolecular film of $DiC_{12}PC$ spreads at an initial surface pressure (π_i) ranging from 4 to 37 mN m^{-1}.

3. Results and discussion

3.1. Preparation of tyrosyl esters

A chemoselective procedure was used to synthesis lipophilic tyrosyl esters (**TyC_2** to **$TyC_{18:1}$**) (Fig. 1). The conversion yields calculated after 120 h of incubation using lipases from *Staphylococcus xylosus* and *Rhizopus oryzae* immobilized onto $CaCO_3$ (SXLi and ROLi, respectively) are presented in Table 1. As it can be seen, using SXLi as biocatalyst, a good ester synthesis yield was obtained when using short acyl chain ester (**TyC_2** and **TyC_3**). For medium and long chain esters (**TyC_8** to **$TyC_{18:1}$**), the conversion yield decrease with the increasing of the acyl chain length. Different results were obtained when using ROLi as biocatalyst. In fact, from **TyC_2** to **TyC_{12}**, the conversion yield increased with the increasing of the acyl chain length. Above 12 carbons, the conversion yield decrease significantly. This difference in the synthesis behavior between the two lipases could be correlated to their hydrolysis selectivity toward the triacylglycerols length chain. In fact, Mosbah et al. [15] have reported that SXL hydrolyse triacylglycerols without significant chain length preference while Ben Saleh et al. [16] have reported that ROL is highly selective for long-chain substrates hydrolysis. Pleiss et al. [22] have reported that in organic medium, the scissile fatty acid binding site is the primary determinant for chain length specificity, while the choice of the reaction conditions is of minor importance. Indeed, lipases which have high activity for short chain fatty acids, have the scissile fatty acid binding site relatively short and have a small hydrophobic area located at the wall of the binding funnel. However, lipases which have relatively low activity for short chain fatty acids, but increasing activity for longer fatty acids have the scissile fatty acid binding site located in a long well-defined hydrophobic crevice. The fatty acid unsaturation seems to affect the synthesis yield. In fact, the conversion yield obtained with the tyrosyl stearate, 51.8%; decreases to 47% when using the oleic acid to synthesize the tyrosyl oleate. Our observations are in agreement with those described by Selmi et al. [23] when synthesizing several triacylglycerol esters using immobilized *Rhizomucor miehei* lipase. These authors concluded that the increase of the unsaturation number is responsible for the lower rate of triacylglycerols synthesis [23].

Table 1
The conversion yields of the tyrosol esters derivatives.

Tyrosyl esters	Radical	Conversion yield (%) after 120 h of reaction time	
		SXLi	ROLi
Tyrosyl acetate (**TyC_2**)	—CH_3	95.08 ± 2.7	20.04 ± 2.4
Tyrosyl propionate (**TyC_3**)	—C_2H_5	83.12 ± 2.0	22.70 ± 2.2
Tyrosyl caprylate (**TyC_8**)	—C_7H_{15}	79.56 ± 2.3	56.80 ± 2.9
Tyrosyl capriate (**TyC_{10}**)	—C_9H_{19}	68.60 ± 1.98	65.13 ± 2.8
Tyrosyl laurate (**TyC_{12}**)	—$C_{11}H_{23}$	60.15 ± 1.89	70.56 ± 2.7
Tyrosyl palmitate (**TyC_{16}**)	—$C_{15}H_{31}$	54.00 ± 2.0	63.08 ± 2.1
Tyrosyl stearate (**TyC_{18}**)	—$C_{17}H_{35}$	51.86 ± 2.1	59.40 ± 2.6
Tyrosyl oleate (**$TyC_{18:1}$**)	—$C_{17}H_{33}$	47.15 ± 2.2	55.80 ± 2.5

3.2. Identification of purified tyrosyl esters

Fig. 2 shows the spectroscopic analysis of TyC_{16} as a typical example of tyrosyl derivatives. HPLC analysis of the reaction mixture after 120 h (Fig. 2A) showed a new peak which corresponds to the tyrosyl palmitate derivative. The purified reaction product was analyzed by HPLC (Fig. 2A) and identified by LC/MS. Many of the esters could be identified tentatively by expected elution order in UV spectra from the individual reactions, but there are several overlapping species that required MS analysis for unequivocal identification. As shown in Fig. 2B, the LC/MS analysis in negative mode of pure tyrosyl palmitate exhibited a molecular ion at m/z = 375.48 $[M-H]^-$ attributed to the molecular weight of ester. The peaks corresponding to ions at m/z = 421.39 $[M+46]^-$ and m/z = 375.48 $[2M]^-$ are attributed respectively to ester linked to a formic acid molecule and a duplicate mass of native ester. The same peaks are found for the other derivatives summarized in the Table 2.

3.3. ABTS assay

The TEAC of the tyrosol and its esters derivatives showed that the radical-scavenging activities of tyrosyl esters are lower than the TEAC of the original tyrosol (data not shown). These results are closed to those previously reported by Mateos et al. [13] showing that the transesterification of tyrosol with aliphatic chain acids decreased their ability to scavenge peroxyl radicals [13].

Table 2
Fragments identified by LC–MS analysis.

Compounds	Characteristics	$[M]^-$	$[M+46]^-$	$[2M]^-$
Ty	Colorless amorphous solid	137.00	183.00	275.00
TyC_2	Colorless oil	179.00	225.00	359.27
TyC_3	Colorless oil	193.07	239.15	287.23
TyC_8	Colorless oil	263.18	309.30	527.46
TyC_{10}	Colorless oil	291.27	337.30	583.54
TyC_{12}	White amorphous solid	319.30	365.35	639.53
TyC_{16}	White amorphous solid	375.48	421.48	751.52
TyC_{18}	White amorphous solid	403.43	449.28	–
$TyC_{18:1}$	Yellow oil	401.48	447.39	–

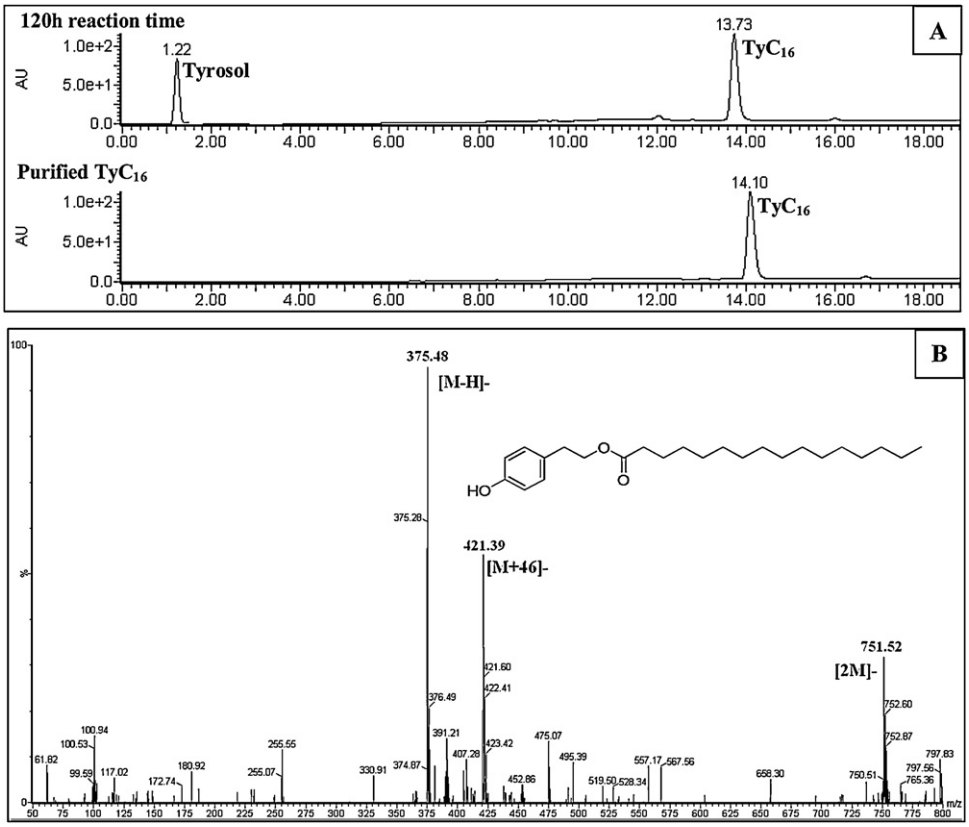

Fig. 2. (A) HPLC profiles of enzymatic esterification mixture of **TyC_{16}** after 120 h of reaction time. (B) LC–MS spectra of purified **TyC_{16}**.

3.4. Force/area curves of tyrosol and its esters

The main parameters which characterize the film state of a given substance spread on an aqueous subphase are the temperature *T*, the surface pressure *Z*, the surface area and the number of molecules. These parameters can be controlled when using the Langmuir film balance system. The properties of monolayers spread at the air/water interface were estimated by recording the isotherms of surface pressure versus the area per molecule. The obtained results allowed us to evaluate the stability of the formed monolayers and to determine the packing and the order of molecules in the air/water interface.

Surface pressure–area isotherms were checked for the pure tyrosol and its derivatives. Fig. 3 gives the surface-pressure dependence as a function of the molecular area on a buffered subphase at pH 8.0. Among the nine tested compounds, only four where able to form a stable monolayer when spread on an aqueous subphase. These compounds are: tyrosyl laurate (**TyC_{12}**), tyrosyl palmitate (**TyC_{16}**), tyrosyl stearate (**TyC_{18}**) and tyrosyl oleate (**$TyC_{18:1}$**). While the tyrosol and its short and meduim chain derivatives cannot be maintained as a stable monolayer on the aqueous subphase due to their dissolution during the compression. The monolayer stability was confirmed by the absence of hysteresis upon compression/decompression (data not shown). As it can be seen in Fig. 3, upon compression of long chain saturated tyrosyl derivatives films (**TyC_{16}** and **TyC_{18}**), the monolayer surface pressure increased slowly and then a sharp decrease was observed. The surface pressure increased to reach a collapse at about 46 mN m^{-1} and 50 mN m^{-1} for **TyC_{16}** and **TyC_{18}**, respectively. This behavior was described as a characteristic of saturated fatty acid.

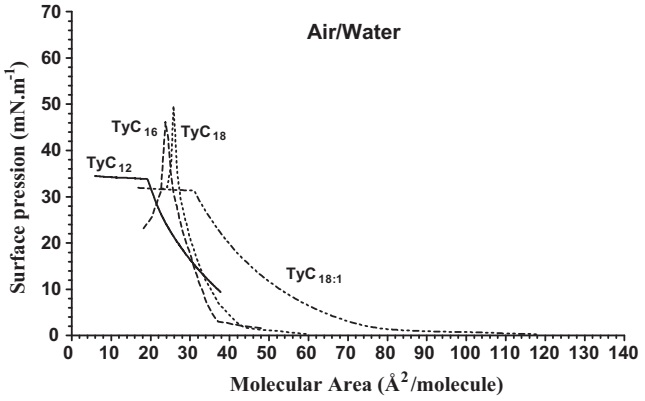

Fig. 3. Surface pressure versus molecular area of monomolecular films of tyrosol and the different tyrosyl derivatives.
—, TyC_{12}; - - - -, **TyC_{16}**; · · ·, **TyC_{18}**; – · · –, **$TyC_{18:1}$**.

Since 1971, Sims and Zografi [24] have studied the monolayer properties of saturated fatty acids and their hydroxylated derivatives. They have reported that, in the plot of the surface pressure of compressed stearic acid film, there is a region of a high surface pressure increase, terminating at a maximum value considered to be the film collapse pressure. This peak is followed by an initial fall in surface pressure despite continued compression, with eventual leveling to a constant surface pressure. As reported by the authors [24], beyond the transition a variety of closer-packing arrangements can take place leading to higher surface pressures. Generally this has been looked upon as a region where fatty acids exhibit different close-packed "two-dimensional solid" arrangements, in a manner analogous to three-dimensional polymorphic crystalline forms [25]. Whatever these arrangements are not stable which lead to the expulsion of molecules from the surface and a corresponding loss in surface pressure. This kind of behavior was seen also with other saturated fatty acids ranging from 15 to 20 carbons in chain

Table 3
Pressure of collapse, molecular area and critical surface pressure (π_c) of the tyrosol and tyrosyl acyl esters.

	Collapse ($mN\,m^{-1}$)	Molecular area ($Å^2$/molecule)	π_c ($DiC_{12}PC$) ($mN\,m^{-1}$)
Ty	0	0	0
TyC_2	0	0	0
TyC_3	0	0	0
TyC_8	0	0	33.09
TyC_{10}	0	0	29.16
TyC_{12}	34.66 ± 0.9	17.47 ± 1.37	45.50
TyC_{16}	46.83 ± 1.16	21.42 ± 1.6	37.15
TyC_{18}	50.34 ± 2.07	23.67 ± 2.13	32.04
$TyC_{18:1}$	31.37 ± 0.05	28.33 ± 1.1	47.65

length [24]. As shown in Table 3, the collapse pressure of TyC_{16} and TyC_{18} are about 46.83 and 50.34 $mN\,m^{-1}$ respectively. These collapse pressures are higher than those reported by Sims and Zografi for palmitic and stearic acids (32 and 49.8 $mN\,m^{-1}$ respectively). The same authors reported that α-hydroxy fatty acids derivatives and their corresponding fatty acids have similar behaviors upon the compression of their films at the air/water interface. Nevertheless, an increase of the collapse pressure values is observed for α-hydroxy fatty acids derivatives. According to these authors, the introduction of α-hydroxy group increases the stability of fatty acids which is most likely due to the interactions of polar group with adjacent polar groups and water which will also play an important role in the expulsion process, and perhaps, the increase of collapse pressure [24].

In this study, different behavior was observed for the unsaturated tyrosyl derivative (**$TyC_{18:1}$**) force/area curves. As shown in Fig. 3, the surface pressure slowly increases to reach a plateau of collapse pressure. This pattern was previously observed with unsaturated fatty acid films and it is a typical shape of liquid lipid monolayers [26].

The addition of tyrosol to the lauric acid (which when spread on an aqueous subphase, forms slightly soluble monolayers [27]) causes to exhibit a stable monolayer. The surface pressure corresponding to the collapse (Π_{coll}) and the molecular areas are summarized in Table 3. We can see, for saturated acyl chain tyrosyl derivatives, the Π_{coll} and the molecular area increases with increasing chain length. However, the unsaturation in the acyl chain of **$TyC_{18:1}$** induces a decrease of the Π_{coll} and an increase of the molecular area (28.33 $Å^2$ for **$TyC_{18:1}$** and 23.67$Å^2$ for **TyC_{18}**). This fact might be explained by a higher steric hindrance upon packing caused by the presence of one unsaturation in the acyl chain of the tyrosyl oleate derivative [26].

3.5. Interactions of Tyrosol derivatives with $DiC_{12}PC$ monolayer

The term 'monolayer penetration' is used to study the interaction of an insoluble monolayer spread at the air/water interface with an active compound injected in the aqueous phase. The interaction is measured by maintaining the film area constant and measuring the surface pressure changes after addition of each compound to the subphase.

In order to study the influence of the length and the nature of the tyrosyl derivatives acyl chain on the adsorption properties of the molecules, we compared their critical surface pressures (π_c) using $DiC_{12}PC$ monolayer. The maximal surface pressure increase was determined at different initial pressures (π_i) of $DiC_{12}PC$ varying from 4 to 37 $mN\,m^{-1}$ (Table 3). The critical surface pressure (π_c) for each ester was estimated by linear extrapolation of the experimental curves at zero surface pressure increase. The value of the maximal surface pressure increase ($\Delta\pi_{max}$) reached at equilibrium (around 20 min after the injection of the tyrosyl

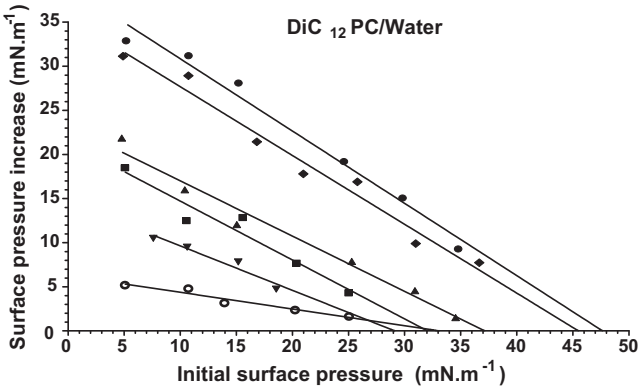

Fig. 4. Maximal increase in surface pressure after tyrosyl derivatives injection with respect to the initial surface pressure of $DiC_{12}PC$ films spread in a cylindrical Teflon trough (volume, 15 mL; surface, 17.42 cm^2). Final tyrosyl derivatives concentration, 0.5 μM. Buffer, 10 mM Tris–HCl, pH 8.0, 100 mM NaCl, 21 mM $CaCl_2$, and 1 mM EDTA. (○) **TyC_8**, (▼) **TyC_{10}**, (♦) **TyC_{12}**, (▲) **TyC_{16}**, (■) **TyC_{18}**, (●) **$TyC_{18:1}$**.

derivative in the aqueous subphase) was determined and plotted as a function of π_i (Fig. 4). For all tyrosyl derivatives, a general trend was observed: higher was π_i, lower was the incorporation of the tyrosyl derivatives into the monolayer because of the higher packing of phospholipids. **Ty**, **TyC_2**, **TyC_3** cannot interact with the $DiC_{12}PC$ film (data not shown). It can be seen from Table 3 that the unsaturation in the acyl chain seems to strengthen the interaction of **$TyC_{18:1}$** with the phospholipid film. In fact, the critical surface pressure of **$TyC_{18:1}$** and **TyC_{18}** are 47.65 $mN\,m^{-1}$ and 32.04 $mN\,m^{-1}$, respectively. Regarding the length of the saturated chain derivatives (**TyC_{12}**, **TyC_{16}** and **TyC_{18}**), one can notice that the interaction of the esters with the $DiC_{12}PC$ monolayers decrease with the increasing of the acyl chain length. In light of these results, if one takes the π_c as a threshold value to appreciate the capacity of the tyrosyl esters to penetrate into a monomolecular films of phospholipid, we can tentatively conclude that the medium and long chain tyrosyl esters (**TyC_8** to **$TyC_{18:1}$**) could interact efficiently with biological membrane, characterized by a surface pressure between 25 and 35 $mN\,m^{-1}$ [28].

4. Conclusion

Different chain lengths fatty acid have been used to synthetize tyrosyl derivatives (from **TyC_2** to **$TyC_{18:1}$**) using a non commercial immobilized lipases (ROLi or SXLi) as a catalyst. The compounds obtained were identified, using mass spectrometry. The study of the interfacial properties of these esters by the monomolecular film technique shows that the esterification of tyrosol by different acyl chains generated lipophilic antioxidants that could penetrate into an oil based cosmetic, food and pharmaceutical products.

Acknowledgements

Our thanks are due to Mr. Massoud Mazari, Mr. Vincent Delorme (PhD Students, Marseille) and Mr. Pavan-Kumar Kamarajugadda (Postdoc, Marseille) for LCMS analysis. This work received financial support from the "Ministry of Higher Education, Scientific Research in Tunisia".

References

[1] C.W. McConlogue, D. Malamud, T.K. Vanderlick, Biochim. Biophys. Acta 1372 (1998) 124–134.
[2] Y. Nagawa, S.L. Regen, J. Am. Chem. Soc. 113 (1991) 7237–7240.
[3] M. Laguerre, L.J. Lopez Giraldo, J. Lecomte, M.C. Figueroa-Espinoza, B. Barea, J. Weiss, E.A. Decker, P. Villeneuve, J. Agric. Food Chem. 58 (2010) 2869–2876.
[4] I. Fki, N. Allouche, S. Sayadi, Food Chem. 93 (2005) 197–204.

[5] D. Caruso, B. Berra, F. Giavarini, N. Cortesi, E. Fedeli, G. Galli, Nutr. Metab. Cardiovasc. Dis. 9 (1999) 102–107.
[6] R. De la Puerta, V. Ruiz-Gutierrez, J.R. Hoult, Biochem. Pharmacol. 57 (1999) 445–449.
[7] C. Giovannini, E. Straface, D. Modesti, E. Coni, A. Cantafora, M. De Vincenzi, W. Malorni, R. Masella, J. Nutr. 129 (1999) 1269–1277.
[8] M.B. Plotnikov, G.A. Chernysheva, V.I. Smol'yakova, M.Y. Maslov, I.V. Cherkashina, A.P. Krysin, I.V. Sorokina, T.G. Tolstikova, Exp. Biol. Med. 143 (2007) 61–63.
[9] G.A. Chernyshova, M.B. Plotnikov, V.I. Smol'yakova, I.V. Golubeva, O.I. Aliev, T.G. Tolstikova, A.P. Krysin, I.V. Sorokina, Bull. Exp. Biol. Med. 143 (2007) 689–691.
[10] D. Vauzour, G. Corona, J.P.E. Spencer, Arch. Biochem. Biophys. 501 (2010) 106–111.
[11] E. Fragopoulou, T. Nomikos, H.C. Karantonis, C. Apostolakis, E. Pliakis, M. Samiotaki, G. Panayotou, S. Antonopoulou, J. Agric. Food Chem. 55 (2007) 80–89.
[12] I. Aissa, M. Bouaziz, H. Ghamgui, A. Kammoun, N. Miled, S. Sayadi, Y. Gargouri, J. Agric, Food Chem. 55 (2007) 10298–10305.
[13] R. Mateos, M. Trujillo, G. Pereira-Caro, A. Madrona, A. Cert, J.L. Espartero, J. Agric. Food Chem. 56 (2008) 10960–10966.
[14] R. Lucas, F. Comelles, D. Alcantra, O.S. Maldonado, M. Curcuroze, J.L. Parra, J.C. Morales, J. Agric. Food Chem. 58 (2010) 8021–8026.
[15] H. Mosbah, A. Sayari, H. Mejdoub, H. Dhouib, Y. Gargouri, Biochim. Biophys. Acta 1723 (2005) 282–291.
[16] A. Ben Salah, K. Fendri, Y. Gargouri, Revue Française Corps Gras 4 (1994) 133–137.
[17] H. Ghamgui, M. Karra-Châabouni, Y. Gargouri, Enzyme Microb. Technol. 35 (2004) 355–363.
[18] J. Rathelot, R. Julien, P. Canioni, C. Coereli, L. Sarda, Biochimie 57 (1975) 1117–1122.
[19] R. Re, N. Pellegrini, A. Proteffente, A. Pannala, M. Yang, C. Rice-Evans, Free Radic. Biol. Med. 26 (1999) 1231–1237.
[20] R. Verger, G.H. de Haas, Chem. Phys. Lipids 10 (1973) 127–136.
[21] G. Piéroni, Y. Gargouri, L. Sarda, R. Verger, Adv. Colloid Interface Sci. 32 (1990) 341–378.
[22] J. Pleiss, M. Fischer, R.D. Schmid, Chem. Phys. Lipids 93 (1998) 67–80.
[23] B. Selmi, E. Gontier, F. Ergan, D. Thomas, Enzyme Microb. Technol. 23 (1998) 182–186.
[24] B. Sims, G. Zografi, Chem. Phys. Lipids 6 (1971) 109–120.
[25] E. Stenhagen, in: Braude, Nachod (Eds.), Determination of Organic Structures by Physical Methods, Academic Press, New York, 1955, p. 325.
[26] K. Hac-Wydro, K. Jedrzejek, P. Dynarowicz-Łatka, Colloids Surf. B 72 (2009) 101–111.
[27] P. Dynarowicz-Łatkaa, A. Dhanabalanb, O.N. Oliveira, Adv. Colloid Interface Sci. 91 (2001) 221–293.
[28] M.J. Sanchez-Martın, I. Haro, M.A. Alsina, M.A. Busquets, M. Pujol, J. Phys. Chem. B 114 (2010) 448–456.